A Search for the Higgs Boson Using Neural Networks in Events with Missing Energy and b-quark Jets in $p\overline{p}$ Collisions at $\sqrt{s} = 1.96$ TeV

T. Aaltonen,[24] J. Adelman,[14] B. Álvarez González[v],[12] S. Amerio[dd],[44] D. Amidei,[35] A. Anastassov,[39] A. Annovi,[20] J. Antos,[15] G. Apollinari,[18] A. Apresyan,[49] T. Arisawa,[58] A. Artikov,[16] J. Asaadi,[54] W. Ashmanskas,[18] A. Attal,[4] A. Aurisano,[54] F. Azfar,[43] W. Badgett,[18] A. Barbaro-Galtieri,[29] V.E. Barnes,[49] B.A. Barnett,[26] P. Barria[ff],[47] P. Bartos,[15] G. Bauer,[33] P.-H. Beauchemin,[34] F. Bedeschi,[47] D. Beecher,[31] S. Behari,[26] G. Bellettini[ee],[47] J. Bellinger,[60] D. Benjamin,[17] A. Beretvas,[18] A. Bhatti,[51] M. Binkley,[18] D. Bisello[dd],[44] I. Bizjak[jj],[31] R.E. Blair,[2] C. Blocker,[7] B. Blumenfeld,[26] A. Bocci,[17] A. Bodek,[50] V. Boisvert,[50] D. Bortoletto,[49] J. Boudreau,[48] A. Boveia,[11] B. Brau[a],[11] A. Bridgeman,[25] L. Brigliadori[cc],[6] C. Bromberg,[36] E. Brubaker,[14] J. Budagov,[16] H.S. Budd,[50] S. Budd,[25] K. Burkett,[18] G. Busetto[dd],[44] P. Bussey,[22] A. Buzatu,[34] K. L. Byrum,[2] S. Cabrera[x],[17] C. Calancha,[32] S. Camarda,[4] M. Campanelli,[31] M. Campbell,[35] F. Canelli[14],[18] A. Canepa,[46] B. Carls,[25] D. Carlsmith,[60] R. Carosi,[47] S. Carrillo[n],[19] S. Carron,[18] B. Casal,[12] M. Casarsa,[18] A. Castro[cc],[6] P. Catastini[ff],[47] D. Cauz,[55] V. Cavaliere[ff],[47] M. Cavalli-Sforza,[4] A. Cerri,[29] L. Cerrito[q],[31] S.H. Chang,[28] Y.C. Chen,[1] M. Chertok,[8] G. Chiarelli,[47] G. Chlachidze,[18] F. Chlebana,[18] K. Cho,[28] D. Chokheli,[16] J.P. Chou,[23] K. Chung[o],[18] W.H. Chung,[60] Y.S. Chung,[50] T. Chwalek,[27] C.I. Ciobanu,[45] M.A. Ciocci[ff],[47] A. Clark,[21] D. Clark,[7] G. Compostella,[44] M.E. Convery,[18] J. Conway,[8] M.Corbo,[45] M. Cordelli,[20] C.A. Cox,[8] D.J. Cox,[8] F. Crescioli[ee],[47] C. Cuenca Almenar,[61] J. Cuevas[v],[12] R. Culbertson,[18] J.C. Cully,[35] D. Dagenhart,[18] M. Datta,[18] T. Davies,[22] P. de Barbaro,[50] S. De Cecco,[52] A. Deisher,[29] G. De Lorenzo,[4] M. Dell'Orso[ee],[47] C. Deluca,[4] L. Demortier,[51] J. Deng[f],[17] M. Deninno,[6] M. d'Errico[dd],[44] A. Di Canto[ee],[47] G.P. di Giovanni,[45] B. Di Ruzza,[47] J.R. Dittmann,[5] M. D'Onofrio,[4] S. Donati[ee],[47] P. Dong,[18] T. Dorigo,[44] S. Dube,[53] K. Ebina,[58] A. Elagin,[54] R. Erbacher,[8] D. Errede,[25] S. Errede,[25] N. Ershaidat[bb],[45] R. Eusebi,[54] H.C. Fang,[29] S. Farrington,[43] W.T. Fedorko,[14] R.G. Feild,[61] M. Feindt,[27] J.P. Fernandez,[32] C. Ferrazza[gg],[47] R. Field,[19] G. Flanagan[s],[49] R. Forrest,[8] M.J. Frank,[5] M. Franklin,[23] J.C. Freeman,[18] I. Furic,[19] M. Gallinaro,[51] J. Galyardt,[13] F. Garberson,[11] J.E. Garcia,[21] A.F. Garfinkel,[49] P. Garosi[ff],[47] H. Gerberich,[25] D. Gerdes,[35] A. Gessler,[27] S. Giagu[hh],[52] V. Giakoumopoulou,[3] P. Giannetti,[47] K. Gibson,[48] J.L. Gimmell,[50] C.M. Ginsburg,[18] N. Giokaris,[3] M. Giordani[ii],[55] P. Giromini,[20] M. Giunta,[47] G. Giurgiu,[26] V. Glagolev,[16] D. Glenzinski,[18] M. Gold,[38] N. Goldschmidt,[19] A. Golossanov,[18] G. Gomez,[12] G. Gomez-Ceballos,[33] M. Goncharov,[33] O. González,[32] I. Gorelov,[38] A.T. Goshaw,[17] K. Goulianos,[51] A. Gresele[dd],[44] S. Grinstein,[4] C. Grosso-Pilcher,[14] R.C. Group,[18] U. Grundler,[25] J. Guimaraes da Costa,[23] Z. Gunay-Unalan,[36] C. Haber,[29] S.R. Hahn,[18] E. Halkiadakis,[53] B.-Y. Han,[50] J.Y. Han,[50] F. Happacher,[20] K. Hara,[56] D. Hare,[53] M. Hare,[57] R.F. Harr,[59] M. Hartz,[48] K. Hatakeyama,[5] C. Hays,[43] M. Heck,[27] J. Heinrich,[46] M. Herndon,[60] J. Heuser,[27] S. Hewamanage,[5] D. Hidas,[53] C.S. Hill[c],[11] D. Hirschbuehl,[27] A. Hocker,[18] S. Hou,[1] M. Houlden,[30] S.-C. Hsu,[29] R.E. Hughes,[40] M. Hurwitz,[14] U. Husemann,[61] M. Hussein,[36] J. Huston,[36] J. Incandela,[11] G. Introzzi,[47] M. Iori[hh],[52] A. Ivanov[p],[8] E. James,[18] D. Jang,[13] B. Jayatilaka,[17] E.J. Jeon,[28] M.K. Jha,[6] S. Jindariani,[18] W. Johnson,[8] M. Jones,[49] K.K. Joo,[28] S.Y. Jun,[13] J.E. Jung,[28] T.R. Junk,[18] T. Kamon,[54] D. Kar,[19] P.E. Karchin,[59] Y. Kato[m],[42] R. Kephart,[18] W. Ketchum,[14] J. Keung,[46] V. Khotilovich,[54] B. Kilminster,[18] D.H. Kim,[28] H.S. Kim,[28] H.W. Kim,[28] J.E. Kim,[28] M.J. Kim,[20] S.B. Kim,[28] S.H. Kim,[56] Y.K. Kim,[14] N. Kimura,[58] L. Kirsch,[7] S. Klimenko,[19] K. Kondo,[58] D.J. Kong,[28] J. Konigsberg,[19] A. Korytov,[19] A.V. Kotwal,[17] M. Kreps,[27] J. Kroll,[46] D. Krop,[14] N. Krumnack,[5] M. Kruse,[17] V. Krutelyov,[11] T. Kuhr,[27] N.P. Kulkarni,[59] M. Kurata,[56] S. Kwang,[14] A.T. Laasanen,[49] S. Lami,[47] S. Lammel,[18] M. Lancaster,[31] R.L. Lander,[8] K. Lannon[u],[40] A. Lath,[53] G. Latino[ff],[47] I. Lazzizzera[dd],[44] T. LeCompte,[2] E. Lee,[54] H.S. Lee,[14] J.S. Lee,[28] S.W. Lee[w],[54] S. Leone,[47] J.D. Lewis,[18] C.-J. Lin,[29] J. Linacre,[43] M. Lindgren,[18] E. Lipeles,[46] A. Lister,[21] D.O. Litvintsev,[18] C. Liu,[48] T. Liu,[18] N.S. Lockyer,[46] A. Loginov,[61] L. Lovas,[15] D. Lucchesi[dd],[44] J. Lueck,[27] P. Lujan,[29] P. Lukens,[18] G. Lungu,[51] J. Lys,[29] R. Lysak,[15] D. MacQueen,[34] R. Madrak,[18] K. Maeshima,[18] K. Makhoul,[33] P. Maksimovic,[26] S. Malde,[43] S. Malik,[31] G. Manca[e],[30] A. Manousakis-Katsikakis,[3] F. Margaroli,[49] C. Marino,[27] C.P. Marino,[25] A. Martin,[61] V. Martin[k],[22] M. Martínez,[4] R. Martínez-Ballarín,[32] P. Mastrandrea,[52] M. Mathis,[26] M.E. Mattson,[59] P. Mazzanti,[6] K.S. McFarland,[50] P. McIntyre,[54] R. McNulty[j],[30] A. Mehta,[30] P. Mehtala,[24] A. Menzione,[47] C. Mesropian,[51] T. Miao,[18] D. Mietlicki,[35] N. Miladinovic,[7] R. Miller,[36] C. Mills,[23] M. Milnik,[27] A. Mitra,[1] G. Mitselmakher,[19] H. Miyake,[56] S. Moed,[23] N. Moggi,[6] M.N. Mondragon[n],[18] C.S. Moon,[28] R. Moore,[18] M.J. Morello,[47] J. Morlock,[27] P. Movilla Fernandez,[18] J. Mülmenstädt,[29] A. Mukherjee,[18] Th. Muller,[27] P. Murat,[18] M. Mussini[cc],[6] J. Nachtman[o],[18] Y. Nagai,[56] J. Naganoma,[56] K. Nakamura,[56] I. Nakano,[41] A. Napier,[57] J. Nett,[60]

C. Neu[z],[46] M.S. Neubauer,[25] S. Neubauer,[27] J. Nielsen[g],[29] L. Nodulman,[2] M. Norman,[10] O. Norniella,[25] E. Nurse,[31] L. Oakes,[43] S.H. Oh,[17] Y.D. Oh,[28] I. Oksuzian,[19] T. Okusawa,[42] R. Orava,[24] K. Osterberg,[24] S. Pagan Griso[dd],[44] C. Pagliarone,[55] E. Palencia,[18] V. Papadimitriou,[18] A. Papaikonomou,[27] A.A. Paramanov,[2] B. Parks,[40] S. Pashapour,[34] J. Patrick,[18] G. Pauletta[ii],[55] M. Paulini,[13] C. Paus,[33] T. Peiffer,[27] D.E. Pellett,[8] A. Penzo,[55] T.J. Phillips,[17] G. Piacentino,[47] E. Pianori,[46] L. Pinera,[19] K. Pitts,[25] C. Plager,[9] L. Pondrom,[60] K. Potamianos,[49] O. Poukhov*,[16] F. Prokoshin[y],[16] A. Pronko,[18] F. Ptohos[i],[18] E. Pueschel,[13] G. Punzi[ee],[47] J. Pursley,[60] J. Rademacker[c],[43] A. Rahaman,[48] V. Ramakrishnan,[60] N. Ranjan,[49] I. Redondo,[32] P. Renton,[43] M. Renz,[27] M. Rescigno,[52] S. Richter,[27] F. Rimondi[cc],[6] L. Ristori,[47] A. Robson,[22] T. Rodrigo,[12] T. Rodriguez,[46] E. Rogers,[25] S. Rolli,[57] R. Roser,[18] M. Rossi,[55] R. Rossin,[11] P. Roy,[34] A. Ruiz,[12] J. Russ,[13] V. Rusu,[18] B. Rutherford,[18] H. Saarikko,[24] A. Safonov,[54] W.K. Sakumoto,[50] L. Santi[ii],[55] L. Sartori,[47] K. Sato,[56] A. Savoy-Navarro,[45] P. Schlabach,[18] A. Schmidt,[27] E.E. Schmidt,[18] M.A. Schmidt,[14] M.P. Schmidt*,[61] M. Schmitt,[39] T. Schwarz,[8] L. Scodellaro,[12] A. Scribano[ff],[47] F. Scuri,[47] A. Sedov,[49] S. Seidel,[38] Y. Seiya,[42] A. Semenov,[16] L. Sexton-Kennedy,[18] F. Sforza[ee],[47] A. Sfyrla,[25] S.Z. Shalhout,[59] T. Shears,[30] P.F. Shepard,[48] M. Shimojima[t],[56] S. Shiraishi,[14] M. Shochet,[14] Y. Shon,[60] I. Shreyber,[37] A. Simonenko,[16] P. Sinervo,[34] A. Sisakyan,[16] A.J. Slaughter,[18] J. Slaunwhite,[40] K. Sliwa,[57] J.R. Smith,[8] F.D. Snider,[18] R. Snihur,[34] A. Soha,[18] S. Somalwar,[53] V. Sorin,[4] P. Squillacioti[ff],[47] M. Stanitzki,[61] R. St. Denis,[22] B. Stelzer,[34] O. Stelzer-Chilton,[34] D. Stentz,[39] J. Strologas,[38] G.L. Strycker,[35] J.S. Suh,[28] A. Sukhanov,[19] I. Suslov,[16] A. Taffard[f],[25] R. Takashima,[41] Y. Takeuchi,[56] R. Tanaka,[41] J. Tang,[14] M. Tecchio,[35] P.K. Teng,[1] J. Thom[h],[18] J. Thome,[13] G.A. Thompson,[25] E. Thomson,[46] P. Tipton,[61] P. Ttito-Guzmán,[32] S. Tkaczyk,[18] D. Toback,[54] S. Tokar,[15] K. Tollefson,[36] T. Tomura,[56] D. Tonelli,[18] S. Torre,[20] D. Torretta,[18] P. Totaro[ii],[55] S. Tourneur,[45] M. Trovato[gg],[47] S.-Y. Tsai,[1] Y. Tu,[46] N. Turini[ff],[47] F. Ukegawa,[56] S. Uozumi,[28] N. van Remortel[b],[24] A. Varganov,[35] E. Vataga[gg],[47] F. Vázquez[n],[19] G. Velev,[18] C. Vellidis,[3] M. Vidal,[32] I. Vila,[12] R. Vilar,[12] M. Vogel,[38] I. Volobouev[w],[29] G. Volpi[ee],[47] P. Wagner,[46] R.G. Wagner,[2] R.L. Wagner,[18] W. Wagner[aa],[27] J. Wagner-Kuhr,[27] T. Wakisaka,[42] R. Wallny,[9] S.M. Wang,[1] A. Warburton,[34] D. Waters,[31] M. Weinberger,[54] J. Weinelt,[27] W.C. Wester III,[18] B. Whitehouse,[57] D. Whiteson[f],[46] A.B. Wicklund,[2] E. Wicklund,[18] S. Wilbur,[14] G. Williams,[34] H.H. Williams,[46] P. Wilson,[18] B.L. Winer,[40] P. Wittich[h],[18] S. Wolbers,[18] C. Wolfe,[14] H. Wolfe,[40] T. Wright,[35] X. Wu,[21] F. Würthwein,[10] A. Yagil,[10] K. Yamamoto,[42] J. Yamaoka,[17] U.K. Yang[r],[14] Y.C. Yang,[28] W.M. Yao,[29] G.P. Yeh,[18] K. Yi[o],[18] J. Yoh,[18] K. Yorita,[58] T. Yoshida[l],[42] G.B. Yu,[17] I. Yu,[28] S.S. Yu,[18] J.C. Yun,[18] A. Zanetti,[55] Y. Zeng,[17] X. Zhang,[25] Y. Zheng[d],[9] and S. Zucchelli[cc6]

(CDF Collaboration†)

[1] *Institute of Physics, Academia Sinica, Taipei, Taiwan 11529, Republic of China*
[2] *Argonne National Laboratory, Argonne, Illinois 60439*
[3] *University of Athens, 157 71 Athens, Greece*
[4] *Institut de Fisica d'Altes Energies, Universitat Autonoma de Barcelona, E-08193, Bellaterra (Barcelona), Spain*
[5] *Baylor University, Waco, Texas 76798*
[6] *Istituto Nazionale di Fisica Nucleare Bologna,* [cc] *University of Bologna, I-40127 Bologna, Italy*
[7] *Brandeis University, Waltham, Massachusetts 02254*
[8] *University of California, Davis, Davis, California 95616*
[9] *University of California, Los Angeles, Los Angeles, California 90024*
[10] *University of California, San Diego, La Jolla, California 92093*
[11] *University of California, Santa Barbara, Santa Barbara, California 93106*
[12] *Instituto de Fisica de Cantabria, CSIC-University of Cantabria, 39005 Santander, Spain*
[13] *Carnegie Mellon University, Pittsburgh, PA 15213*
[14] *Enrico Fermi Institute, University of Chicago, Chicago, Illinois 60637*
[15] *Comenius University, 842 48 Bratislava, Slovakia; Institute of Experimental Physics, 040 01 Kosice, Slovakia*
[16] *Joint Institute for Nuclear Research, RU-141980 Dubna, Russia*
[17] *Duke University, Durham, North Carolina 27708*
[18] *Fermi National Accelerator Laboratory, Batavia, Illinois 60510*
[19] *University of Florida, Gainesville, Florida 32611*
[20] *Laboratori Nazionali di Frascati, Istituto Nazionale di Fisica Nucleare, I-00044 Frascati, Italy*
[21] *University of Geneva, CH-1211 Geneva 4, Switzerland*
[22] *Glasgow University, Glasgow G12 8QQ, United Kingdom*
[23] *Harvard University, Cambridge, Massachusetts 02138*
[24] *Division of High Energy Physics, Department of Physics, University of Helsinki and Helsinki Institute of Physics, FIN-00014, Helsinki, Finland*
[25] *University of Illinois, Urbana, Illinois 61801*
[26] *The Johns Hopkins University, Baltimore, Maryland 21218*

[27]Institut für Experimentelle Kernphysik, Karlsruhe Institute of Technology, D-76131 Karlsruhe, Germany
[28]Center for High Energy Physics: Kyungpook National University,
Daegu 702-701, Korea; Seoul National University, Seoul 151-742,
Korea; Sungkyunkwan University, Suwon 440-746,
Korea; Korea Institute of Science and Technology Information,
Daejeon 305-806, Korea; Chonnam National University, Gwangju 500-757,
Korea; Chonbuk National University, Jeonju 561-756, Korea
[29]Ernest Orlando Lawrence Berkeley National Laboratory, Berkeley, California 94720
[30]University of Liverpool, Liverpool L69 7ZE, United Kingdom
[31]University College London, London WC1E 6BT, United Kingdom
[32]Centro de Investigaciones Energeticas Medioambientales y Tecnologicas, E-28040 Madrid, Spain
[33]Massachusetts Institute of Technology, Cambridge, Massachusetts 02139
[34]Institute of Particle Physics: McGill University, Montréal, Québec,
Canada H3A 2T8; Simon Fraser University, Burnaby, British Columbia,
Canada V5A 1S6; University of Toronto, Toronto, Ontario,
Canada M5S 1A7; and TRIUMF, Vancouver, British Columbia, Canada V6T 2A3
[35]University of Michigan, Ann Arbor, Michigan 48109
[36]Michigan State University, East Lansing, Michigan 48824
[37]Institution for Theoretical and Experimental Physics, ITEP, Moscow 117259, Russia
[38]University of New Mexico, Albuquerque, New Mexico 87131
[39]Northwestern University, Evanston, Illinois 60208
[40]The Ohio State University, Columbus, Ohio 43210
[41]Okayama University, Okayama 700-8530, Japan
[42]Osaka City University, Osaka 588, Japan
[43]University of Oxford, Oxford OX1 3RH, United Kingdom
[44]Istituto Nazionale di Fisica Nucleare, Sezione di Padova-Trento, [dd]University of Padova, I-35131 Padova, Italy
[45]LPNHE, Universite Pierre et Marie Curie/IN2P3-CNRS, UMR7585, Paris, F-75252 France
[46]University of Pennsylvania, Philadelphia, Pennsylvania 19104
[47]Istituto Nazionale di Fisica Nucleare Pisa, [ee]University of Pisa,
[ff]University of Siena and [gg]Scuola Normale Superiore, I-56127 Pisa, Italy
[48]University of Pittsburgh, Pittsburgh, Pennsylvania 15260
[49]Purdue University, West Lafayette, Indiana 47907
[50]University of Rochester, Rochester, New York 14627
[51]The Rockefeller University, New York, New York 10021
[52]Istituto Nazionale di Fisica Nucleare, Sezione di Roma 1,
[hh]Sapienza Università di Roma, I-00185 Roma, Italy
[53]Rutgers University, Piscataway, New Jersey 08855
[54]Texas A&M University, College Station, Texas 77843
[55]Istituto Nazionale di Fisica Nucleare Trieste/Udine,
I-34100 Trieste, [ii]University of Trieste/Udine, I-33100 Udine, Italy
[56]University of Tsukuba, Tsukuba, Ibaraki 305, Japan
[57]Tufts University, Medford, Massachusetts 02155
[58]Waseda University, Tokyo 169, Japan
[59]Wayne State University, Detroit, Michigan 48201
[60]University of Wisconsin, Madison, Wisconsin 53706
[61]Yale University, New Haven, Connecticut 06520

(Dated: November 18, 2009)

We report on a search for the standard model Higgs boson produced in association with a W or Z boson in $p\overline{p}$ collisions at $\sqrt{s} = 1.96$ TeV recorded by the CDF II experiment at the Tevatron in a data sample corresponding to an integrated luminosity of $2.1\,\mathrm{fb}^{-1}$. We consider events which have no identified charged leptons, an imbalance in transverse momentum, and two or three jets where at least one jet is consistent with originating from the decay of a b hadron. We find good agreement between data and predictions. We place 95% confidence level upper limits on the production cross section for several Higgs boson masses ranging from 110 GeV/c^2 to 150 GeV/c^2. For a mass of 115 GeV/c^2 the observed (expected) limit is 6.9 (5.6) times the standard model prediction.

PACS numbers: 14.80.Bn,13.85.Rm

[*]Deceased

[†]With visitors from [a]University of Massachusetts Amherst,

The Higgs boson is the last particle of the standard model (SM) of particle physics that remains to be discovered. The existence of the Higgs boson is expected to be the direct physical manifestation of the mechanism that provides mass to fundamental particles [1]. Expectations from electroweak data collected at the Tevatron, LEP, and SLD indirectly constrain the Higgs boson mass to $m_H < 157\,\mathrm{GeV}/c^2$ at 95% confidence level (C.L.) [2]. Direct searches at LEP have excluded $m_H < 114.4\,\mathrm{GeV}/c^2$ at 95% C.L. [3]. Upper limits on the production cross section from searches in the region $110 < m_H < 135\ \mathrm{GeV}/c^2$ remain well above the standard model prediction [2], and greatly benefit from improvements of the experimental sensitivity. In this mass region, $b\bar{b}$ is the main decay mode. The b quarks fragment into jets of hadrons, and the signal can be reconstructed as a resonance in the invariant mass distribution of the two jets. The CDF and D0 collaborations perform searches for the low mass Higgs boson (H) produced in association with a vector boson V ($V = W$, Z), since the requirement of a charged lepton or of large missing transverse energy from the decay of a vector boson dramatically reduces the backgrounds from multi-jet processes.

This Letter presents a search for the standard model VH associated production in events with b-quark jets and large missing transverse energy with data corresponding to an integrated luminosity of $2.1\,\mathrm{fb}^{-1}$. This analysis significantly increases the acceptance for signal with respect to previous Tevatron searches [4, 5] and introduces advanced analysis methods. We consider ZH production, where $Z \to \nu\bar{\nu}$ and the neutrinos (ν) escape detection, or $Z \to \ell\ell$ when both charged leptons (ℓ) are undetected or are identified as jets. For WH production we are sensitive to events where $W \to e\nu$ or $W \to \tau\nu$ when the charged lepton is identified as a jet, and $W \to \ell\nu$ when ℓ is undetected. Critical challenges for this analysis are to achieve a high signal-to-background ratio and to model the multi-jet background production accurately. We employ artificial neural networks (ANNs) [6] to improve the event selection and signal discrimination and implement a novel data-driven determination of the multi-jet background.

CDF II is a multipurpose detector that is described in detail elsewhere [7, 8]. Charged particle tracking is performed with silicon microstrip detectors surrounded by a cylindrical wire drift chamber. A superconducting solenoid provides a 1.4 T axial magnetic field in the tracking volume for momentum measurements. Segmented sampling calorimeters surround the solenoid, measure energies of interacting particles, and determine each event's missing transverse energy, $\not\!\!E_{\mathrm{T}}$ [8]. A system of drift chambers and scintillation counters outside the calorimeters detects muon candidates [7]. Jets are reconstructed from energy depositions in the calorimeter towers using a jet clustering cone algorithm [9] with a cone size of radius $\Delta R = \sqrt{(\Delta\phi)^2 + (\Delta\eta)^2} = 0.4$. Corrections are applied to account for effects that can cause mismeasurement of the jet energies, such as non-linear and non-uniform calorimeter response, energy loss in the uninstrumented detector regions, and multiple interactions [9]. Jet energies are further corrected using momentum measurements provided by the tracker, using a method similar to that described in [10]. The more precise measurement of the jet energies improves the candidate Higgs boson mass resolution by $\approx 10\%$ and increases the signal acceptance by $\approx 10\%$. Both the magnitude and direction of $\not\!\!E_{\mathrm{T}}$ are recomputed after the jet energies are corrected.

The events used in this search are selected by a three-level trigger system. The level 1 trigger requires $\not\!\!E_{\mathrm{T}} \geq 25$ GeV , where the $\not\!\!E_{\mathrm{T}}$ is determined using calorimeter trigger towers with $E_{\mathrm{T}} > 1\,\mathrm{GeV}$. The level 2 trigger adds the requirement that there be two jet clusters of $E_{\mathrm{T}} > 10\,\mathrm{GeV}$, one of which in the region $|\eta| < 1.1$. The level 3 trigger adds the requirement that $\not\!\!E_{\mathrm{T}} > 35\,\mathrm{GeV}$. Previous studies found that this trigger becomes fully efficient only at high values of the $\not\!\!E_{\mathrm{T}}$ and of the two leading jets' transverse energies [4]. After offline reconstruction, the event selection requires $\not\!\!E_{\mathrm{T}} > 50\,\mathrm{GeV}$, and the transverse energies $E_{\mathrm{T}}^{J_1}$ and $E_{\mathrm{T}}^{J_2}$ of the two jets with the highest transverse energy, J_1 and J_2 ("leading jets"), satisfy the conditions $E_{\mathrm{T}}^{J_1} > 35\,\mathrm{GeV}$ and $E_{\mathrm{T}}^{J_2} > 25\,\mathrm{GeV}$. We consider an event to have three jets if the E_{T} of the third leading jet, J_3, is greater than 15 GeV. Events with four or more jets with $E_{\mathrm{T}} > 15\,\mathrm{GeV}$ and $|\eta| < 2.4$ are rejected. Events passing these criteria are denoted as the "pre-tagged" sample. After these selections, the expected signal-to-background ratio is around 1/20 000.

Amherst, Massachusetts 01003, [b]Universiteit Antwerpen, B-2610 Antwerp, Belgium, [c]University of Bristol, Bristol BS8 1TL, United Kingdom, [d]Chinese Academy of Sciences, Beijing 100864, China, [e]Istituto Nazionale di Fisica Nucleare, Sezione di Cagliari, 09042 Monserrato (Cagliari), Italy, [f]University of California Irvine, Irvine, CA 92697, [g]University of California Santa Cruz, Santa Cruz, CA 95064, [h]Cornell University, Ithaca, NY 14853, [i]University of Cyprus, Nicosia CY-1678, Cyprus, [j]University College Dublin, Dublin 4, Ireland, [k]University of Edinburgh, Edinburgh EH9 3JZ, United Kingdom, [l]University of Fukui, Fukui City, Fukui Prefecture, Japan 910-0017 [m]Kinki University, Higashi-Osaka City, Japan 577-8502 [n]Universidad Iberoamericana, Mexico D.F., Mexico, [o]University of Iowa, Iowa City, IA 52242, [p]Kansas State University, Manhattan, KS 66506 [q]Queen Mary, University of London, London, E1 4NS, England, [r]University of Manchester, Manchester M13 9PL, England, [s]Muons, Inc., Batavia, IL 60510, [t]Nagasaki Institute of Applied Science, Nagasaki, Japan, [u]University of Notre Dame, Notre Dame, IN 46556, [v]University de Oviedo, E-33007 Oviedo, Spain, [w]Texas Tech University, Lubbock, TX 79609, [x]IFIC(CSIC-Universitat de Valencia), 56071 Valencia, Spain, [y]Universidad Tecnica Federico Santa Maria, 110v Valparaiso, Chile, [z]University of Virginia, Charlottesville, VA 22906 [aa]Bergische Universität Wuppertal, 42097 Wuppertal, Germany, [bb]Yarmouk University, Irbid 211-63, Jordan [jj]On leave from J. Stefan Institute, Ljubljana, Slovenia,

We veto events with at least one high-$p_{\rm T}$ isolated electron or muon [11], deliberately using fairly loose lepton identification criteria. A muon candidate is defined as any isolated track with $|\eta| < 1.0$ and $p_{\rm T} > 10$ GeV/c that leaves energy in the calorimeters consistent with a minimum ionizing particle, where the isolation requirement is that the total energy in a cone of size 0.4 around the track is less than 10% of the track momentum. Candidate electrons are identified by clustered energy deposits in the electromagnetic calorimeter with $E_{\rm T} > 10\,{\rm GeV}$ that have an electromagnetic to hadronic energy ratio and a shower shape compatible with electrons and are associated to an isolated track.

In the mass range probed in this Letter, the SM Higgs boson decays predominantly to b-quark pairs; thus, large backgrounds originating from light-flavor jet production can be reduced by identifying b jets in the candidate events. Due to their relatively long lifetime, b and c hadrons can travel a few millimeters from the primary vertex before decaying into lighter hadrons. Jets originating from a b quark can be identified ("tagged") by the SECVTX algorithm [12], which reconstructs vertices that are significantly displaced from the $p\bar{p}$ interaction point, and the JETPROB algorithm [13], which classifies jets using the probability that tracks within the jet are consistent with originating from the primary vertex. To enhance the expected signal significance we subdivide the sample into three independent categories: events with two jets tagged by SECVTX (SV+SV), events with one jet tagged by SECVTX and another by JETPROB (SV+JP) and events with only one jet tagged by SECVTX (SV).

The selected sample is dominated by background from the production of multi-jet (MJ), top quark (pair and electroweak production), W or Z plus jets, and WW, WZ or ZZ events. Significant $\not\!\!E_{\rm T}$ in multi-jet events appears when b quarks decay semileptonically or when jet energies are mismeasured. In both cases $\vec{\not\!\!E}_{\rm T}$ is often aligned with $\vec{E}_{\rm T}^{J_2}$. Therefore, events with $\Delta\phi(\vec{\not\!\!E}_{\rm T}, \vec{E}_{\rm T}^{J_2}) < 0.4$, no identified leptons, and $50 < \not\!\!E_{\rm T} < 70\,{\rm GeV}$ are used to measure the rates with which the heavy-flavor jets (h.f., originating from a b or c quark) from multi-jet production and light flavor jets mistakenly identified as b jets ("mistags") are tagged. The tagging rate (TR) is parametrized as a function of $H_{\rm T}$ [8] of the event and $E_{\rm T}$, η, and ζ of the jet. The observable ζ is defined as $\zeta = c\sum_i p^i_{\rm T,track}/E_{\rm T}$ where $p^i_{\rm T,track}$ includes tracks within a jet with a significant impact parameter and $0.5 < p^i_{\rm T,track} < 200$ GeV/c. Jets originating from b quarks are expected to have a large ζ. The multi-jet background in the single (double) tagged sample is determined by the probability to tag one (two) jet(s) from the pre-tagged (single-tagged) sample [11]. When applying the tagging rate to the data we avoid double counting the contributions due to other backgrounds by applying the TR parametrization to all Monte Carlo (MC) simulated data and subtracting their contribution from the multi-jet background. The validity of the tagging rate modeling is verified in various control regions, which are defined below. The remaining backgrounds are estimated using PYTHIA [14] simulations, and single top production is simulated with MADEVENT [15]. The signal MC samples are generated with PYTHIA. The normalizations of the MC samples are described in [11].

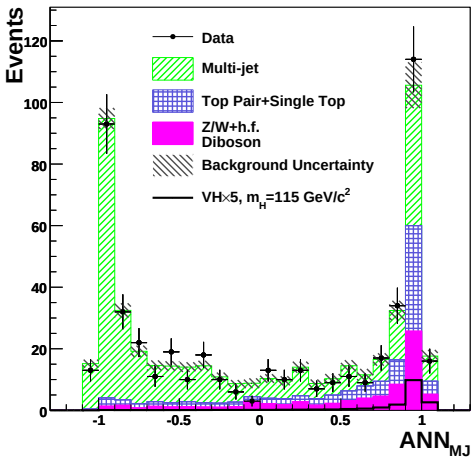

FIG. 1: The distribution of $\mathrm{ANN_{MJ}}$ for double-tagged events.

We start the selection of the signal region by requiring no identified charged leptons, $\not\!\!E_{\rm T} > 50\,{\rm GeV}$, $\Delta\phi(\vec{\not\!\!E}_{\rm T}, \vec{E}_{\rm T}^{J_1}) \geq 1.5$, and $\Delta\phi(\vec{\not\!\!E}_{\rm T}, \vec{E}_{\rm T}^{J_{2,3}}) \geq 0.4$. These selection criteria remove $\approx$10% of the signal in the pretag sample while reducing the backgrounds by approximately an order of magnitude. We employ an ANN, denoted as $\mathrm{ANN_{MJ}}$, using kinematic variables to separate signal from multi-jet background. To discriminate against events with $\not\!\!E_{\rm T}$ due to mismeasurements in the calorimeter, we use the momentum imbalance in the tracker, $\not\!\!P_{\rm T}^{\rm tr}$ [8]. The magnitude of $\not\!\!E_{\rm T}$, $\not\!\!P_{\rm T}^{\rm tr}$, the angle between them, the azimuthal angles between $\not\!\!E_{\rm T}$, $\not\!\!P_{\rm T}^{\rm tr}$ and the jet directions, and several other less discriminating variables are used as inputs to $\mathrm{ANN_{MJ}}$ [11]. The distribution of $\mathrm{ANN_{MJ}}$ is shown in Fig. 1. The $\mathrm{ANN_{MJ}}$ peaks at 1 for the signal, while the background from multi-jet production peaks at -1. Selecting events with $\mathrm{ANN_{MJ}} \geq 0$ rejects over 50% of the total background and retains 95% of the signal. This region is defined as the signal region and is analyzed for the presence of the Higgs boson signal.

In order to avoid potential bias in the search, we test our understanding of the SM background in several control regions. The control region called EWK, sensitive to electroweak processes and top production, contains events with at least one lepton and $\Delta\phi(\vec{\not\!\!E}_{\rm T}, \vec{E}_{\rm T}^{J_2}) \geq 0.4$. We also define several control regions dominated by multi-jet processes where we have no identified lep-

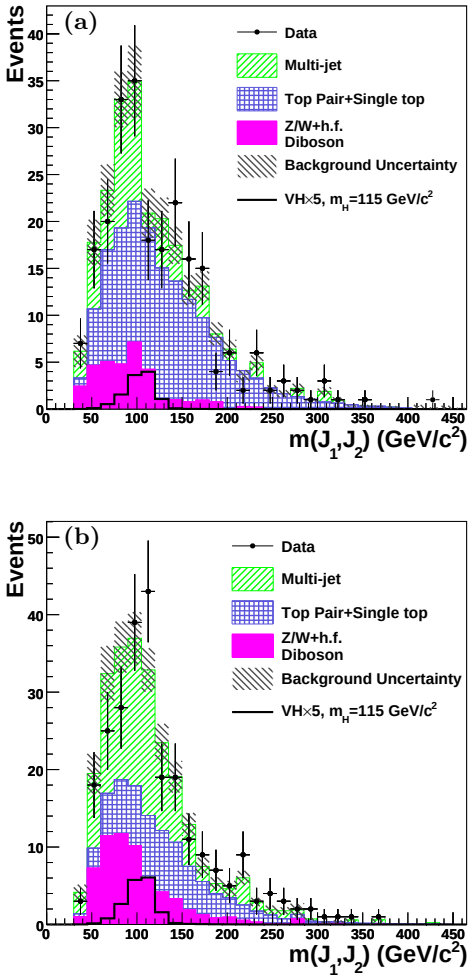

FIG. 2: Dijet invariant mass distribution for double-tagged events in (a) EWK control regions, and in (b) signal region.

TABLE I: Comparison of the total number of expected and observed events in the signal region for different b-tagging categories. The uncertainties contain both MC statistical error and systematic uncertainties.

Process	SV+SV or SV+JP	SV
Multi-jet	120.1 ± 21.3	941.2 ± 86.0
Single Top	15.7 ± 3.0	43.2 ± 7.9
Top Pair	54.5 ± 7.9	124.5 ± 17.0
Di-boson	9.2 ± 1.8	35.6 ± 6.8
W + h.f.	32.0 ± 14.7	296.9 ± 129.5
Z + h.f.	22.1 ± 11.5	107.0 ± 45.8
Total Prediction	254 ± 39	1548.4 ± 168.1
Observed	253	1443
Expected Signal for m_H=115 GeV/c^2		
$ZH \to \nu\nu bb$	1.8 ± 0.2	2.1 ± 0.2
$WH \to (\ell)\nu bb$	1.6 ± 0.2	1.8 ± 0.2
$ZH \to (\ell\ell)bb$	0.07 ± 0.01	0.09 ± 0.01

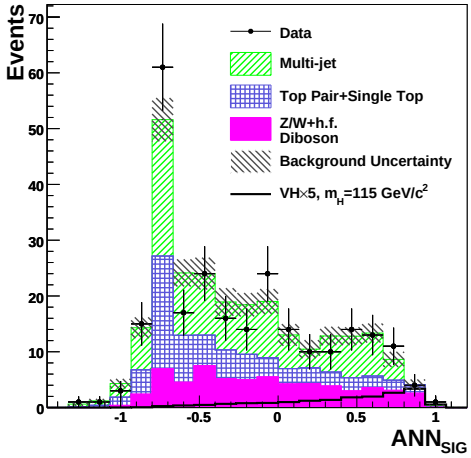

FIG. 3: The distribution of $\mathrm{ANN_{sig}}$ for double-tagged events.

tons. The region denoted as MJ1 contains events with $\Delta\phi(\vec{\not\!\!E}_{\rm T}, \vec{E}_{\rm T}^{J_2}) < 0.4$ and $\not\!\!E_{\rm T} \geq 70\,\mathrm{GeV}$. The region denoted as MJ2 contains events with $\Delta\phi(\vec{\not\!\!E}_{\rm T}, \vec{E}_{\rm T}^{J_1}) \geq 1.5$, $\Delta\phi(\vec{\not\!\!E}_{\rm T}, \vec{E}_{\rm T}^{J_{2,3}}) \geq 0.4$, and $\mathrm{ANN_{MJ}} < -0.5$. The predictions of the multi-jet background are tested in MJ1 and MJ2. The distributions of kinematic variables, such as the invariant mass of the two leading jets $m(J_1, J_2)$, have been found to be in agreement with observations in the control regions [11], as shown in Fig.2(a).

To achieve a greater separation between signal and background we deploy a second ANN, denoted as $\mathrm{ANN_{sig}}$, for discriminating the remaining backgrounds from the expected signal. Since the background fraction and composition are different for events with two or three jets we train the $\mathrm{ANN_{sig}}$ separately for these categories. The outputs of the two $\mathrm{ANN_{sig}}$ are combined into a single discriminant for each tagging category. The $\mathrm{ANN_{sig}}$ is trained for several values of m_H. Six input variables are used in $\mathrm{ANN_{sig}}$: the invariant mass of the two leading jets $m(J_1, J_2)$ (Fig. 2), the invariant mass of the $\not\!\!E_{\rm T}$ and all jets, $H_{\rm T} - \not\!\!E_{\rm T}$, $\not\!\!H_{\rm T} - \not\!\!E_{\rm T}$, TRACKMET [16] and the maximum $\Delta R(\vec{E}_{\rm T}^{J_i}, \vec{E}_{\rm T}^{J_k})$. The variable TRACKMET is the output of a ANN developed using tracking information to enhance the separation of events with real $\not\!\!E_{\rm T}$. The most discriminating variable of the $\mathrm{ANN_{sig}}$ is $m(J_1, J_2)$.

The distribution of $\mathrm{ANN_{sig}}$ is shown in Fig. 3 for double-tagged events. The number of signal and background events after the final selection are shown in Table I. Since no significant excess is observed, we compute 95% C.L. upper limits for the Higgs boson production cross section times the branching fraction $B(H \to b\bar{b})$. For m_H=115 GeV/c^2 we expect a total of 4.0 (3.5) signal events with one (two) b-tagged jets [17].

We analyze the binned $\mathrm{ANN_{sig}}$ discriminant distribution to test for a WH or ZH signal in the presence of SM backgrounds. The systematic uncertainties included

TABLE II: The combined 95% C.L. upper limits on cross section times $H \to b\bar{b}$ branching fraction when the Higgs boson is produced in association with a weak vector boson. The last two columns give the ratio of the expected and observed limits with respect to the SM cross section.

m_H (GeV/c^2)	Expected (pb)	Observed (pb)	Ratio Expected	Ratio Observed
110	1.3	1.5	$4.9^{+2.1}_{-1.4}$	5.8
115	1.2	1.5	$5.6^{+2.4}_{-1.6}$	6.9
120	1.2	1.5	$7.2^{+2.9}_{-2.1}$	8.9
130	1.0	1.4	$10.3^{+4.3}_{-2.9}$	14.4
140	0.9	1.0	$18.6^{+7.8}_{-5.4}$	21.0
150	0.8	1.0	$43.3^{+19.0}_{-12.4}$	49.8

in the calculation are classified as correlated (uncorrelated) depending on if they do (do not) affect both signal and the background processes [11, 16]. The uncorrelated systematic uncertainties are the following: multi-jet normalization (20.6% in SV+SV, 15.6% in SV+JP and 5.5% in SV categories) and MC statistical fluctuations. Additionally we assign the following uncertainties due to cross sections: 15.9% and 15.2% to single top in s- and t-channels, 8.6% to top pair, 11.5% to diboson and 40% to W + h.f. and Z + h.f. The statistical variations in the determination of the TR can also modify the shape of the kinematic distributions. The shapes obtained by varying the TR probabilities by $\pm 1\sigma$ are applied as systematic uncertainties to each bin of $\mathrm{ANN_{sig}}$. The correlated systematic uncertainties are the following: luminosity measurement (6.0%), b-tagging efficiency scale factor between data and MC (8.6% for SV+SV, 12.4% for SV+JP and 4.3% for SV), trigger efficiency (<3%), lepton veto efficiency (2%), parton distribution function uncertainty (2%) and 3.8-13.0% for jet energy scale (JES) [9]. We also assign systematic uncertainties on the shape of $\mathrm{ANN_{sig}}$ due to JES and trigger efficiency uncertainties. Initial- and final-state-radiation systematic uncertainties (between 1% and 5%) are applied to the signal predictions.

Including all the uncertainties, the expected and observed upper limits at the 95% C.L. on VH production cross section times branching fraction $Br(H \to b\bar{b})$ are shown in Table II. Expected limits are obtained by generating pseudo-experiments from the expected SM $\mathrm{ANN_{sig}}$ shapes to calculate the median ZH and WH contribution which could be excluded at the 95% C.L. in the zero signal hypothesis. The limits are computed using the Bayesian likelihood method [18] with a flat prior probability for the signal cross section and Gaussian priors for the uncertainties on acceptance and backgrounds. We combine the search channels SV+SV, SV+JP, and SV by taking the product of their likelihoods and simultaneously varying the correlated uncertainties. The observed limits agree with the expected ones.

In summary, we have performed a direct search for the SM Higgs boson decaying into b-jet pairs using data with integrated luminosity of $2.1\,\mathrm{fb}^{-1}$ accumulated in Run II by the CDF II detector. We use ANNs to separate the signal from the multi-jet and other backgrounds and achieve significant improvements in Higgs boson sensitivity over previous analyses in this decay mode [4]. Distributions of the observed event kinematics and $\mathrm{ANN_{sig}}$ show no significant excess over the background predicted by the SM. The combination of all improvements described above increases the sensitivity of this search by a factor of three with respect to [4], which is a factor of two better than would be expected from the increased luminosity alone.

We thank the Fermilab staff and the technical staffs of the participating institutions for their vital contributions. This work was supported by the U.S. Department of Energy and National Science Foundation; the Italian Istituto Nazionale di Fisica Nucleare; the Ministry of Education, Culture, Sports, Science and Technology of Japan; the Natural Sciences and Engineering Research Council of Canada; the National Science Council of the Republic of China; the Swiss National Science Foundation; the A.P. Sloan Foundation; the Bundesministerium für Bildung und Forschung, Germany; the World Class University Program, the National Research Foundation of Korea; the Science and Technology Facilities Council and the Royal Society, UK; the Institut National de Physique Nucleaire et Physique des Particules/CNRS; the Russian Foundation for Basic Research; the Ministerio de Ciencia e Innovación, and Programa Consolider-Ingenio 2010, Spain; the Slovak R&D Agency; and the Academy of Finland.

[1] P. W. Higgs, Phys. Lett. **12**, 132 (1964).
[2] LEP-Tevatron-SLD Electroweak Working Group, arXiv:0811.4682; Tevatron New Phenomena and Higgs Working Group, arXiv:0903.4001, and references therein.
[3] R. Barate *et al.* (LEP Working Group for Higgs boson searches), Phys. Lett. B **565**, 61 (2003).
[4] T. Aaltonen *et al.* (CDF Collaboration), Phys. Rev. Lett. **100**, 211801 (2008).
[5] T. Abazov *et al.* (D0 Collaboration), Phys. Rev. Lett. **101**, 251802 (2008).
[6] K. Hornik, M. B. Stinchcombe, and H. White, Neural Networks **2**, 359 (1989).
[7] D. Acosta *et al.* (CDF Collaboration), Phys. Rev. D **71**, 032001 (2005).
[8] CDF uses a cylindrical coordinate system with the z axis along the proton beam axis. Pseudorapidity is $\eta = -\ln(\tan(\frac{\theta}{2}))$, where θ is the polar angle, and ϕ is the azimuthal angle relative to the proton beam direction, while $p_{\mathrm{T}} = p\sin\theta$, $E_{\mathrm{T}} = E\sin\theta$. The $\not\!\!E_{\mathrm{T}}$ is defined as the magnitude of $\vec{\not\!\!E}_{\mathrm{T}} = -\sum_i E^i_{\mathrm{T}}\hat{n}_i$, where $\hat{n}_i$ is a unit vector perpendicular to the beam axis and pointing at

the i^{th} calorimeter tower, and $E_{\rm T}^i$ is the transverse energy therein. The scalar sum of transverse energies of the leading jets is denoted as $H_{\rm T}$, and the vector sum of jet $E_{\rm T}$'s is denoted as $\not\!\!H_{\rm T}$. The $\not\!\!\vec{p}_{\rm T}^{\rm tr}$ is defined as negative vector sum of track $p_{\rm T}$'s.

[9] A. Bhatti *et al.*, Nucl. Instrum. Methods A **566**, 375 (2006), and references therein.

[10] C. Adloff *et al.* (H1 Collaboration), Z. Phys. C **74** (1997) 221.

[11] A. Apresyan, Ph.D. Thesis, Purdue University, FERMILAB-THESIS-2009-09.

[12] D. Acosta *et al.* (CDF Collaboration), Phys. Rev. D **71**, 052003 (2005).

[13] A. Abulencia *et al.* (CDF Collaboration), Phys. Rev. D **74**, 072006 (2006).

[14] T. Sjostrand *et al.*, Comput. Phys. Commun. **135**, 238 (2001).

[15] J. Alwall *et al.*, J. High Energy Phys. 09 (2007) 028.

[16] B. S. Parks, Ph.D. Thesis, The Ohio State University, FERMILAB-THESIS-2008-18.

[17] T. Han and S. Willenbrock, Phys. Lett. B **273**, 167 (1991). A. Djouadi, J. Kalinowski, and M. Spira, Comput. Phys. Commun. **108**, 56 (1998).

[18] J. Heinrich *et al.*, arXiv:physics/0409129.